

# Constraints on Possible Singularities for the Unsteady Transonic Small Disturbance (UTSD) Equations

IRENE M. GAMBA

*Department of Mathematics and TICAM*

*The University of Texas at Austin*

RODOLFO R. ROSALES

*Massachusetts Institute of Technology*

AND

ESTEBAN G. TABAK

*Courant Institute*

## Abstract

We discuss the singular behavior of solutions to two-dimensional, general second-order, uniformly elliptic equations in divergence form, with bounded measurable coefficients and discontinuous Dirichlet data along a portion of a Lipschitz boundary. We show that the conjugate to the solution develops a singularity that is at least logarithmic along the boundary at the points of discontinuity in the boundary data.

A problem like this arises in the study of self-similar solutions to the hyperbolic conservation laws in two space dimensions given by the *unsteady transonic small disturbance* (UTSD) flow equations. These solutions model the reflection of a weak shock wave upon a thin wedge in the regime where the von Neumann paradox applies.

The present result provides a step in the direction of understanding the nature of the solutions to the UTSD equations near a triple point. It shows that the flow behind the triple point cannot be strictly subsonic under some mild assumptions on the solutions. © 1999 John Wiley & Sons, Inc.

## 1 Introduction

In this paper, we use a theorem on harmonic measure theory to restrict the type of singularities that the self-similar solutions to the unsteady transonic small disturbance (UTSD) flow equations may support. These constraints replace a previously promising explanation of the von Neumann paradox of Mach reflection. Our main theorem shows that the conormal derivative along the boundary (of a solution to a two-dimensional boundary value problem with discontinuous Dirichlet data for a strictly elliptic symmetric equation in divergence form) has an average at least of  $O(1)$  on any interval  $(t, 2t)$  with a size that depends only on the ellipticity. Here  $t$  is the distance to the discontinuity, and the statement is true for any sufficiently small  $t$ . This implies that the conjugate variable exhibits at least logarithmic behavior along the boundary in a neighborhood of the point of discontinuity. As explained in Section 3, this then rules out such solutions as not physical.

The paper is divided into four sections and an appendix. In Section 2 we present the main theorem for general, second-order, symmetric, uniformly elliptic equations in divergence form, with bounded measurable coefficients in a Lipschitz domain. In Section 3 we explain the relationship of this theorem to the von Neumann paradox and exhibit a class of exact solutions to the (nonlinear) UTSD equations with a fan and a logarithmic singularity. The equations in the natural physical variables are not symmetric, but we exhibit here variables in which the problem takes a symmetric form. In Section 4 we prove the main theorem. The appendix contains some results from harmonic analysis and estimates used in the proofs.

*Remark 1.1.* Our proof depends on two results in harmonic measure theory of elliptic operators in divergence form: the *doubling property of the harmonic measure* and the *boundary Harnack principle*. In the symmetric case these results were proved by Caffarelli, Fabes, Mortola, and Salsa [4]. Recently Kenig, Koch, Pipher, and Toro [11] pointed out that the proofs can be reproduced for nonsymmetric operators in divergence form. In this case, our proof here can be extended to the nonsymmetric case as well.

## 2 A Theorem on Harmonic Measures

We shall describe the behavior of the solutions to a second-order, uniformly elliptic, symmetric equation in divergence form, with bounded measurable coefficients in a two-dimensional Lipschitz domain, when the data has a jump discontinuity at a boundary point.

We begin with a simple example, provided by any harmonic function  $u$  in the half disc.

$$(2.1) \quad D^+ = \{x_1^2 + x_2^2 \leq 1, x_2 > 0\},$$

with boundary data  $u(x_1, 0) = 1$  for  $x_1 < 0$  and  $u(x_1, 0) = 0$  for  $x_1 > 0$ . Near the origin, the function  $u$  behaves asymptotically as  $\theta/\pi$ , where  $\theta$  is the polar angle. Therefore, the normal derivative to the boundary  $u_{x_2}(x_1, 0)$  behaves as  $1/(\pi x_1)$ . It follows that, if  $v = v(x_1, x_2)$  is the harmonic conjugate to  $u$ , then  $v_{x_1}(x_1, 0) \sim -1/(\pi x_1)$ . Thus

$$|v(x_1, 0)| \sim -\frac{1}{\pi} \log |x_1|.$$

That is, if a harmonic function jumps along the boundary, then its harmonic conjugate has a logarithmic singularity at the point of discontinuity.

With the same domain and boundary conditions, consider a bounded function  $\sigma$  satisfying a uniformly elliptic symmetric equation in divergence form. That is,<sup>1</sup>

$$(2.2) \quad \mathcal{L}\sigma = D_i a_{ij} D_j \sigma = \operatorname{div}(A \nabla \sigma) = 0,$$

---

<sup>1</sup>We use  $D_i$  to indicate the partial derivative with respect to  $x_i$ . We also use the convention of summing over repeated indices. Finally, a superscript  $\mathsf{T}$  on a vector or a matrix indicates the transpose.

where the  $2 \times 2$  matrix of coefficients  $A = A(x_1, x_2) = (a_{ij})$  is bounded, measurable, symmetric, and, for some constant  $0 < M \leq 1$ ,

$$(2.3) \quad M|\vec{\zeta}|^2 \leq \vec{\zeta}^\top A(\vec{x})\vec{\zeta} \leq \frac{1}{M}|\vec{\zeta}|^2$$

for any  $\vec{x} = (x_1, x_2)^\top$  in  $D^+$  and any  $\vec{\zeta}$  in  $\mathbb{R}^2$ .

Let now  $\hat{n}$  be the inner unit normal to the domain along the boundary  $\partial D^+$ . Then the inner conormal derivative associated with the operator  $\mathcal{L} = \operatorname{div} A \nabla$  above is given by

$$(2.4) \quad D_\nu = \hat{n}^\top A \nabla.$$

The conormal derivative is defined in such a way that, when equation (2.2) is written as a first-order system (see equation (2.6) below),  $D_\nu \sigma$  coincides with the tangential derivative of the conjugate variable  $\eta$  along the boundary.

We will then prove the following ‘‘averaging’’ theorem:

**THEOREM 2.1** *Consider a solution  $\sigma$  of (2.2) in the domain and with boundary conditions as in (2.1). Let  $\sigma$  be bounded and between 0 and 1. Let  $\sigma_\nu = D_\nu \sigma$  be the inner conormal along the bottom part of the boundary  $x_2 = 0$ , i.e.,  $\sigma_\nu = \{a_{21}\sigma_{x_1} + a_{22}\sigma_{x_2}\} |_{x_2=0}$ . Then there exists a constant  $C > 0$  such that, for any  $\lambda$  with  $0 < |\lambda| < 1$ ,*

$$(2.5) \quad \rho_\lambda = \int_{\lambda/2}^\lambda \sigma_\nu(x_1, 0) dx_1 \geq C.$$

The constant  $C$  depends only on the ellipticity of the operator  $L$  above in (2.2) and (2.3). That is,  $C = C(M)$  only.

Translating this theorem to systems, we have the following, more general result:

**THEOREM 2.2** *Let  $\sigma$  and  $\eta$  satisfy a uniformly elliptic system in  $D^+$*

$$(2.6) \quad \left. \begin{aligned} a_{11}\sigma_{x_1} + a_{12}\sigma_{x_2} &= \eta_{x_2} \\ a_{21}\sigma_{x_1} + a_{22}\sigma_{x_2} &= -\eta_{x_1} \end{aligned} \right\}$$

where the coefficients satisfy the same conditions as above in (2.2) and (2.3). Suppose that the boundary data for  $\sigma$  is Hölder continuous except for a jump discontinuity at the origin of coordinates. Then  $\eta$  goes to infinity at least logarithmically along the boundary as the origin is approached.

Uniform ellipticity is invariant under bi-Lipschitz transformations; thus we have the following:

**COROLLARY 2.3** *In Theorem 2.2, the half disc  $D^+$  can be replaced by any Lipschitz domain, where the solution  $\sigma$  of (2.6) satisfies Dirichlet boundary data that are Hölder continuous except for a jump discontinuity at some point. Then the theorem holds near the point of discontinuity, with  $\eta$  going to infinity along the boundary (at least logarithmically) as the point of discontinuity is approached.*

### 3 The von Neumann Paradox of Oblique Shock Reflection

#### 3.1 Description of the Problem

The problem that motivated this work is the so-called von Neumann paradox, concerning a weak shock wave reflecting upon a very thin wedge. This problem has been investigated theoretically by von Neumann [14, 18, 19], Morawetz [13], Brio and Hunter [3], Čanić and Keyfitz [5, 6], Tabak and Rosales [17], and many others. We describe this paradox briefly here. The reader interested in a more complete description should check the references above, the numerical work of Colella and Henderson [7], and, in a broader context, the experimental work of Sturtevant and Kulkarny [16] and the experimental and numerical work by Glaz, Colella, Glass, and Deschambault [8].

Figure 3.1(a) schematically depicts a straight shock running parallel to a wall and hitting a wedge. We model the dynamics of this problem with the Euler equations of inviscid gas dynamics. These are invariant under stretching of the independent coordinates. The same applies to the configuration in Figure 3.1(a), which we can adopt as the initial conditions for the followup flow. Thus the solution to the problem (after the time  $t = 0$  of Figure 3.1(a)) depends only on the self-similar variables  $x/t$  and  $y/t$  (where  $x$  and  $y$  are the space coordinates measuring distance along and from the wedge wall, respectively). We will make use of this fact below.

The flow configuration for  $t > 0$  depends critically on the strength of the incoming shock and the angle of the wedge. For moderate strengths and relatively large angles, a pattern of *regular reflection* arises, whereby a reflected shock restores to zero the component of the velocity normal to the wedge. For strong shocks and relatively small angles, a *Mach reflection* takes place. In this, the incoming and reflected shocks detach from the wedge, to which they are then joined by a much stronger shock, the *Mach stem*. At the triple point where the three shocks meet, a slip line appears, dividing the domain behind the reflected shock and the Mach stem into two regions with different states.

The situation we are interested in, depicted in Figure 3.1(b), takes place for an intermediate range of parameters (weak shocks and very small angles, the angle scaling as the square root of the shock strength). Under these conditions, numerical calculations and experiments show a reflection pattern that looks very much like a Mach reflection. However, no slip line appears, and the state behind the “Mach stem” is remarkably nonhomogeneous. This configuration is somewhat paradoxical, since the Euler equations of inviscid gas dynamics do not admit, in principle, solutions with three sufficiently weak shocks meeting at a point.

In order to study this paradoxical reflection, one may simplify the equations by magnifying the vicinity of the triple point, using the knowledge of the longitudinal and transversal scales for which the paradox takes place and the fact that the shocks are weak. This leads to a multiple-scale asymptotic expansion (see, for instance,

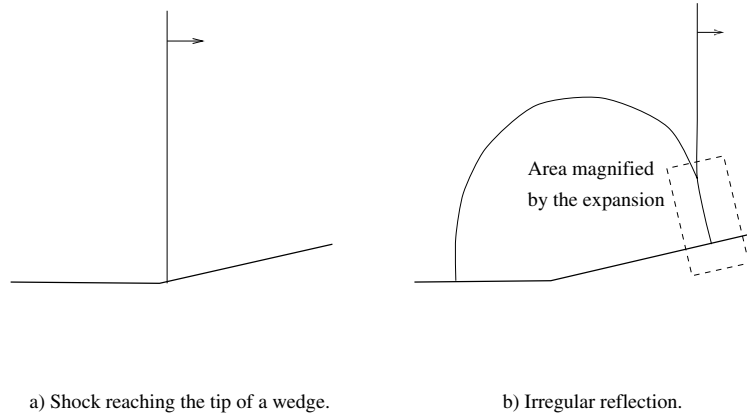


FIGURE 3.1. Irregular reflection of a weak shock wave.

[10] or [15]) yielding the leading-order system of equations

$$(3.1) \quad \left. \begin{aligned} \sigma_t + \left(\frac{1}{2}\sigma^2\right)_x + \eta_y &= 0 \\ \sigma_y - \eta_x &= 0 \end{aligned} \right\}.$$

The independent variables here are stretched by the small shock-strength parameter  $\varepsilon$ . In terms of properly nondimensionalized and unstretched space  $(X, Y)$  and time  $T$  coordinates, we have:  $x = (X - cT)/\varepsilon$ ,  $y = Y/\sqrt{\varepsilon}$ , and  $t = T$ , where  $c$  is the speed of sound in the unperturbed state. The dependent variable  $\sigma$  is proportional to the leading  $(O(\varepsilon))$  perturbation terms in the expansions for the pressure, density, temperature, and velocity parallel to the wedge wall. On the other hand,  $\eta$  represents the leading  $(O(\varepsilon^{3/2}))$  term in the expansion for the component of the velocity normal to the wedge.

In this asymptotic context, the initial data of Figure 3.1(a) become

$$(3.2) \quad (\sigma, \eta) = \begin{cases} (0, 0) & \text{for } x > \alpha y \\ (\sigma_1, -\alpha\sigma_1) & \text{for } x < \alpha y. \end{cases}$$

An oblique shock with angle specified by its cotangent  $\alpha$  moves into a state at rest, hitting a rigid wall described by the no-flow boundary condition  $\eta = 0$ . The intensity of the shock is measured by the value  $\sigma_1$  of  $\sigma$  behind it; the value  $\eta_1 = -\alpha\sigma_1$  follows from the jump conditions across the shock. Using the symmetry of the problem mentioned above, we introduce the self-similar variables

$$\xi = \frac{x}{t} \quad \text{and} \quad \tau = \frac{y}{t}.$$

Then the system of equations (3.1) reduces to

$$(3.3) \quad \left. \begin{aligned} -\xi\sigma_\xi - \tau\sigma_\tau + \left(\frac{1}{2}\sigma^2\right)_\xi + \eta_\tau &= 0 \\ \sigma_\tau - \eta_\xi &= 0 \end{aligned} \right\}.$$

This system has the characteristics

$$\frac{d\xi}{d\tau} = -\frac{\tau}{2} \pm \sqrt{\frac{\tau^2}{4} + \xi - \sigma}.$$

Thus equations (3.3) are of mixed type: hyperbolic when  $\frac{1}{4}\tau^2 + \xi - \sigma > 0$  and elliptic otherwise. The *sonic line* is defined by  $\frac{1}{4}\tau^2 + \xi - \sigma = 0$ .

The paradox mentioned earlier then follows from the following observations:

1. Equations (3.1) with initial data (3.2) do not allow regular reflection when the parameter  $s = \sigma_1/\alpha^2$  is greater than  $\frac{1}{2}$ . In fact, regular reflection in a strict sense cannot arise for values of  $s$  greater than  $2/(2 + \sqrt{5}) = 0.4721$ , the *sonic point*. This follows from a straightforward computation (see, for example, [17]).
2. (Experimental) For  $s$  larger than about  $\frac{1}{2}$ , three shocks are observed apparently meeting at a point. This configuration appears in actual experiments with weak shocks, even though very few physical experiments have  $s$  in the required range [7, 18], in the numerical solution of the full Euler equations of gas dynamics [1], and in the numerical solution of the asymptotic equations (3.1) [17].
3. The asymptotic equations (3.1) do not admit three shocks separating three continuous states. This theorem is proved, for example, in section (IV–B) of [17]. The same result for the equations describing potential flow is proved in [13]. The result also holds for the full equations of gas dynamics.
4. For values of the parameter  $s$  ranging between  $\frac{1}{2}$  and 2, under some weak assumptions, the solution to equations (3.1) with the initial condition (3.2) has to give rise to three shocks intersecting. This result is proved in section (IV–c) of [17]. In particular, if the self-similar equations (3.3) are strictly elliptic in the domain behind the reflected wave, the result that triple shocks arise follows immediately.
5. (Numerical) The most refined numerical experiments to date, performed both for the full Euler equations of gas dynamics by M. Berger [1] and by Rosales and Tabak for the asymptotic equations (3.1), have failed to detect any hyperbolic (supersonic) domain behind the reflected wave.

Thus there is a completely inexplicable contradiction between theory and experiments, and even an apparent inconsistency within the theory alone. Attempting a way out of this paradox, two of the authors here suggested (in [17]) that perhaps there were three shocks after all, but that one of the states separating them was not continuous. In particular, it would be enough if  $\sigma$ ,  $\eta$ , or both could develop a (singular) fanlike structure behind the triple point, thus making all five observations above consistent.

Such fans do exist in the hyperbolic domain of equations (3.3); they are given by simple waves. When the equations become elliptic, however, simple waves are no longer allowed and, for fans to exist, one of the variables has to grow without

bound. But  $\sigma$  must be bounded, as can be shown theoretically in a number of ways and is also apparent in all numerical computations.<sup>2</sup> Thus, if one variable is to grow without bound at the triple point, it had better be  $\eta$ . Such solutions with a fan in  $\sigma$  and a logarithmic singularity in  $\eta$  exist; an exact family is computed below in Section 3.2. On the other hand, a local growth of  $\eta$  near the triple point vaguely resembling (at least qualitatively) a logarithm has been observed in numerical experiments with very fine grids [17]. But such solutions bring in another problem: In order to satisfy the jump conditions,  $\eta$  has to be bounded along the shocks.

Two of the authors conjectured (in [17]) a way out of this paradox, which would have  $\eta$  growing without bound (as the triple point is approached) only within some wedge but not along either the reflected shock or the Mach stem. The main theorem in this paper (coupled with the observation in Remark 3.1 below that the system (3.3) can be written in symmetric form) shows that, if this is to be the case, the equations behind the triple point cannot remain strictly elliptic.

### 3.2 A Family of Exact Solutions with a Fanlike Singularity

Since the self-similar Euler equations have locally centered simple waves, we may expect the USTD equations to have some kind of distorted fanlike solutions. Here we describe a family of exact solutions to equations (3.3) with a singularity at an arbitrary point  $(\xi_0, \tau_0)$ . The Galilean invariance of the equations can be used to choose  $\xi_0 = 0$ . The sign of  $\frac{1}{4}\tau^2 + \xi - \sigma$  determines whether a solution is locally elliptic or hyperbolic. Applying this criterion at the critical point, we replace  $\sigma$  by  $\sigma - \frac{1}{4}\tau_0^2$ , whose sign determines the local character of the equations. We still call the new variable  $\sigma$  to avoid introducing new names. The system (3.3) then becomes

$$(3.4) \quad \left. \begin{aligned} (\frac{1}{4}\tau_0^2 - \xi)\sigma_\xi - \tau\sigma_\tau + \sigma\sigma_\xi + \eta_\tau &= 0 \\ \sigma_\tau - \eta_\xi &= 0 \end{aligned} \right\}.$$

We introduce polar coordinates centered at  $(0, \tau_0)$ . We represent the angle  $\theta$  by its cotangent  $\psi$ , which has a natural interpretation as the characteristic slope  $d\xi/d\tau$ . Thus let

$$(3.5) \quad \psi = \frac{\xi}{\tau - \tau_0} \quad \text{and} \quad \rho = \sqrt{\xi^2 + (\tau - \tau_0)^2}.$$

In these variables, the system in (3.4) becomes

$$(3.6) \quad \begin{aligned} (1 + \psi^2) \left( \left( \sigma + \tau_0\psi + \frac{1}{4}\tau_0^2 \right) \sigma_\psi - \psi\eta_\psi \right) \\ + \rho \left( \left( \left( \frac{1}{4}\tau_0^2 + \sigma \right) \psi - \tau_0 \right) \sigma_\rho + \eta_\rho \right) - \rho^2 \sqrt{1 + \psi^2} \sigma_\rho = 0, \end{aligned}$$

$$(3.7) \quad (1 + \psi^2) (\psi\sigma_\psi + \eta_\psi) - \rho (\sigma_\rho - \psi\eta_\rho) = 0.$$

---

<sup>2</sup>Note that  $\sigma$  determines the speed of sound. An unbounded  $\sigma$  would be physically meaningless.

We will restrict our attention to solutions where  $\sigma$  does not depend on  $\rho$ . In addition, we further simplify the equations by replacing them by two of their linear combinations, namely,  $[(3.6) + \psi(3.7)]$  and  $[\psi(3.6) - (3.7)]$ . Thus

$$(3.8) \quad \left( \sigma + \left( \psi + \frac{1}{2}\tau_0 \right)^2 \right) \sigma_\psi + \rho \eta_\rho = 0,$$

$$(3.9) \quad \psi \left( \left( \sigma + \left( \psi + \frac{1}{2}\tau_0 \right)^2 \right) - (1 + \psi^2) \right) \sigma_\psi - (1 + \psi^2) \eta_\psi = 0.$$

By cross-differentiation, it follows that  $\eta_{\psi\rho} = 0$ , so that

$$(3.10) \quad \eta(\rho, \psi) = \eta_1(\rho) + \eta_2(\psi).$$

Then equations (3.8) and (3.9) reduce to the ODEs

$$(3.11) \quad \rho \eta_1'(\rho) = c,$$

$$(3.12) \quad \left( \sigma + \left( \psi + \frac{1}{2}\tau_0 \right)^2 \right) \sigma'(\psi) = -c,$$

$$(3.13) \quad \eta_2'(\psi) = -c\psi \frac{\sigma + \tau_0\psi + \frac{1}{4}\tau_0^2 - 1}{\left( \sigma + \left( \psi + \frac{1}{2}\tau_0 \right)^2 \right) (1 + \psi^2)},$$

where  $c$  is an arbitrary constant. Two different cases arise, depending on whether  $c$  equals 0 or not.

*Case 1.  $c = 0$*  Then equation (3.11) shows that  $\eta$  does not depend on  $\rho$ . Thus both  $\eta$  and  $\sigma$  are functions of the same single variable  $\psi$ , and we are dealing with a *simple wave*. From equation (3.12), we get

$$(3.14) \quad \sigma = - \left( \psi + \frac{1}{2}\tau_0 \right)^2,$$

so  $\sigma$  is nonpositive. Thus the solution lies in the hyperbolic domain. Finally, it follows from (3.13), after using (3.12) and (3.14) to remove the 0/0 on the right-hand side, that

$$(3.15) \quad \eta = \frac{2}{3} \left( \psi + \frac{1}{2}\tau_0 \right)^3 - \frac{1}{2}\tau_0 \left( \psi + \frac{1}{2}\tau_0 \right)^2 + d,$$

where  $d$  is another arbitrary constant. The solution in (3.14) and (3.15) is the fan emanating from a point already computed in equation (12) of [17].

*Case 2.  $c \neq 0$*  Then, from equation (3.11),  $\eta$  grows logarithmically as  $\rho$  goes to zero:

$$(3.16) \quad \eta_1 = c \log \rho + d,$$

for  $d$  a constant. It now turns out that equation (3.12) is exactly solvable. To see this, take

$$s = \frac{\sigma}{c^{2/3}} \quad \text{and} \quad \Psi = \frac{1}{c^{1/3}} \left( \psi + \frac{1}{2}\tau_0 \right)$$



as the independent and dependent variables, respectively. A Riccati equation follows:

$$\Psi' + \Psi^2 + s = 0.$$

Linearizing with the substitution

$$\Psi = \frac{\omega'(s)}{\omega(s)}$$

yields Airy’s equation

$$(3.17) \quad w''(s) + sw = 0.$$

Thus the solution to equation (3.12) is given by the implicit formula

$$(3.18) \quad \psi + \frac{1}{2}\tau_0 = c^{1/3}\omega'\left(\frac{\sigma}{c^{2/3}}\right)\left(\omega\left(\frac{\sigma}{c^{2/3}}\right)\right)^{-1},$$

where  $w(s)$  is any solution to Airy’s equation. Notice that a *locally elliptic solution*, with  $\sigma > 0$ , corresponds to the oscillatory domain of the Airy functions, while a *locally hyperbolic solution*, with  $\sigma < 0$ , corresponds to the domain where the Airy functions behave exponentially.

Summarizing, we have built a family of exact solutions to the equations where  $\sigma$  depends only on the angle in polar coordinates. Except for the hyperbolic simple wave case ( $c = 0$ ) in these solutions, the variable  $\eta$  grows logarithmically with the distance to the origin of coordinates. The conjecture by two of the authors [17] mentioned at the end of the previous subsection can be rephrased as follows: Can an “elliptic” solution somewhat like the ones in this section for  $c \neq 0$  be constructed so that the logarithmic growth in  $\eta$  will be restricted to a wedge (with  $\eta$  bounded outside this wedge)? Such a solution would play—in the context of weak shock reflection at grazing incidence—the same role slip lines play for “regular” Mach stem, triple-point structures. The theorems in this paper show that this is not possible, at least if one imposes some mild restrictions on the nature of the solution (mainly, uniform ellipticity and a bounded measurable  $\sigma$  near the triple point; see the next subsection).

### 3.3 Relationship to the General Setting

In this section we will show in detail how the UTSD problem described in the prior subsection is a particular case of the general setup of the theorems in Section 2. We will also make a few comments regarding the possible significance of our results for the von Neumann paradox problem.

System (3.3) can be written in the following divergence form:

$$(3.19) \quad \mathcal{L}\sigma = \operatorname{div}(A(\sigma, \vec{x})\nabla\sigma) = 0,$$

where  $\vec{x} = (x_1, x_2)^T = (\xi, \tau)^T$  and the matrix  $A$  is given by

$$(3.20) \quad A = \begin{pmatrix} \sigma - x_1 & -x_2 \\ 0 & 1 \end{pmatrix}.$$

This system is not in symmetric form. However, in Remark 3.1 we show that it can be transformed to a symmetric form by a very simple transformation. Thus the results of Section 2 can be used in this context. Nevertheless, the variables for the symmetric form do not have a natural physical interpretation. Thus we do our presentation here in terms of the form above, where the connection with the actual physical problem is easy to visualize.

Consider now the region  $\Omega$  behind the reflected shock and the Mach stem, as observed in the experiments, for the situation described earlier in Section 3.1. This region is bounded by the reflected shock, the Mach stem—these two intersecting at the triple point  $\vec{x}_0 = (\xi_0, \tau_0)^T$ —and the wall.<sup>3</sup> We concentrate now on the vicinity of the triple point and *assume* that there is some neighborhood of  $\vec{x}_0$  where the *equations are uniformly elliptic*—in fact, *the numerical experiments suggest that this is true for all of  $\Omega$  as defined above!* Thus we *assume* that there exists a neighborhood  $B$  of  $\vec{x}_0$  and a constant  $0 < M \leq 1$  such that  $\sigma$  is measurable in  $B$  and, for any  $\vec{x} = (x_1, x_2)$  in  $B$  and any  $\vec{\zeta}$  in  $R^2$ ,

$$(3.21) \quad M|\vec{\zeta}|^2 \leq \vec{\zeta}^T A(\vec{x})\vec{\zeta} \leq \frac{1}{M}|\vec{\zeta}|^2.$$

Clearly, this is equivalent to

$$(3.22) \quad |\sigma(\vec{x})| \leq K \quad \text{and} \quad \sigma(\vec{x}) > \frac{1}{4}x_2^2 + x_1 + c_M$$

for any  $\vec{x}$  in  $B$  where  $K$  and  $c_M$  are positive constants. Then the operator  $\mathcal{L}$  in (3.19) satisfies the requirements of the theorems in Section 2, using the result in Remark 3.1.

We now focus on the triple point  $\vec{x}_0$ , which belongs to  $\partial B$ , and *assume* that, in a neighborhood of it,

- $\partial B$  is the graph of a Lipschitz function (in some system of coordinates),
- on one side ( $\partial B^-$ , to the “left”) of  $\vec{x}_0$ ,  $\sigma$  has Hölder-continuous boundary values

$$(3.23) \quad \sigma(\vec{x}) = f_1(\vec{x})$$

that converge to  $f^- = f_1(\vec{x}_0)$  at the triple point,

- on the other side ( $\partial B^+$ , to the “right”) of  $\vec{x}_0$ ,  $\sigma$  also has Hölder-continuous boundary values

$$(3.24) \quad \sigma(\vec{x}) = f_2(\vec{x}),$$

which converge to  $f^+ = f_2(\vec{x}_0)$  at the triple point, and

- we have (this inequality actually determines what is right and left above):

$$f^+ - f^- > 0.$$

---

<sup>3</sup>See Figure 3.1(b). The region extends to infinity in the stretched coordinates of equations (3.1)–(3.3).

Note that the numerical calculations suggest that the right side corresponds to the Mach stem, which is the strongest shock in the picture.

These *hypotheses lead to a contradiction* via the main theorem in this paper: A logarithmic singularity in  $\eta$  at the triple point is not compatible with the shock jump conditions for a structure as assumed here. Thus at least one of them must be false. The most likely candidate seems to be the uniform ellipticity in equation (3.22) above. Otherwise, the solution would be forced to be quite singular, as all the other hypotheses above are regularity conditions. While the numerical evidence points quite strongly against the existence of an hyperbolic “pocket” behind the triple point,<sup>4</sup> it is not so clear-cut as to the possibility of the flow being sonic right there. A direct numerical check of this is quite hard, and there is little positive evidence for it in the most refined numerical calculations available to us.

*Remark 3.1.* The similarity form for the equations in the variables that arise naturally from physical considerations, namely (3.3), is not symmetric. However, we point out here that *a simple transformation can reduce the equations to symmetric (in fact, diagonal) form*. Instead of taking  $\vec{x} = (\xi, \tau)^T$  as in equations (3.19) and 3.20, let now:

$$(3.25) \quad x_1 = \xi + \frac{1}{4}\tau^2 \quad \text{and} \quad x_2 = \tau.$$

Then, in terms of the new dependent variables

$$(3.26) \quad \mathcal{S} = \sigma + \frac{1}{2}x_1 + \frac{1}{4}x_2^2 \quad \text{and} \quad \mathcal{N} = \frac{1}{2}x_2(\sigma - x_1) - \eta,$$

the system of equations (3.3) takes the simple form

$$(3.27) \quad \left. \begin{aligned} (\sigma - x_1)\mathcal{S}_{x_1} &= \mathcal{N}_{x_2} \\ \mathcal{S}_{x_2} &= -\mathcal{N}_{x_1} \end{aligned} \right\}$$

where  $\sigma - x_1 = \mathcal{S} - \frac{1}{2}x_1 - \frac{1}{4}x_2^2$ . Notice that the transformation is, in fact, not only smooth but also invertible.

### 4 Proofs of the Theorems

In this section, we prove Theorems 2.1 and 2.2.

#### 4.1 Proof of Theorem 2.1.

The first observation we make is that the semiannular region

$$(4.1) \quad Sr(d) = \left\{ \frac{1}{2}d \leq r \leq d, x_2 \geq 0 \right\},$$

where  $d > 0$  and  $r = \sqrt{x_1^2 + x_2^2}$  can be rescaled to the standard region  $Sr(2)$ , corresponding to  $d = 2$ . This can be done by the transformation (see Figure 4.1)

---

<sup>4</sup>Further, analytical plausibility arguments based on the behavior and propagation of simple waves for the system (3.3) can be made that also suggest that a hyperbolic region is not possible.

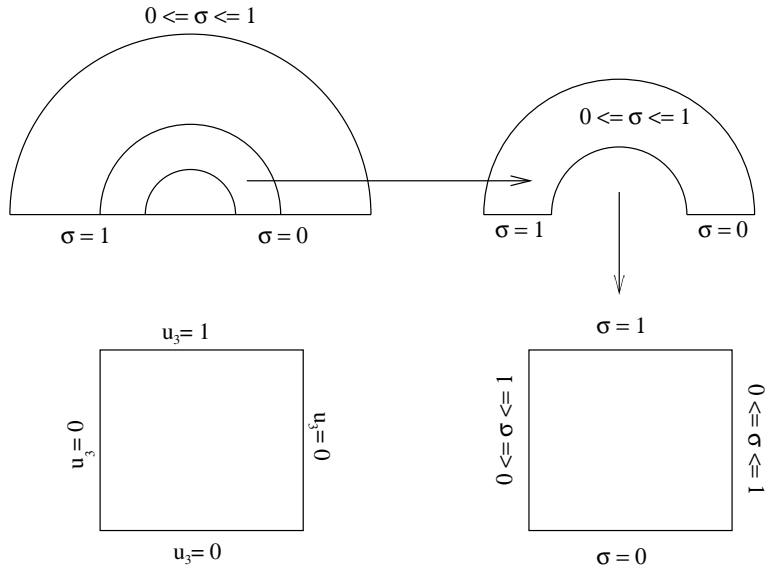


FIGURE 4.1. Map from a semiannular region into a fixed square and comparison with a solution with simpler data.

$\vec{x} \rightarrow (2/d)\vec{x}$ . We note that this map preserves all the properties of the equation and data (including symmetry) with no change in the constant  $M$  in (2.3). The integral in (2.5) is invariant.

Next, we observe that  $Sr(2)$  is bi-Lipschitz equivalent to the unit square

$$(4.2) \quad S_1 = \{0 \leq x_1 \leq 1, 0 \leq x_2 \leq 1\},$$

via the map  $\vec{x} \rightarrow (r - 1, (1/\pi)\theta)^T$  (see Figure 4.1). Again, the properties of the equation and data are preserved (including symmetry) and the integral in (2.5) is invariant.

By the maximum principle,  $\sigma$  is bounded between 0 and 1 in all of  $D^+$ . For any  $0 < |\lambda| < 1$ , consider the region  $Sr(d)$  for  $d = |\lambda|$  and map it into the unit square  $S_1$  as above. In this region  $\sigma$  satisfies the boundary data:

$$(4.3) \quad \sigma = 0 \quad \text{on } x_2 = 0 \quad \text{and} \quad \sigma = 1 \quad \text{on } x_2 = 1,$$

with  $0 < \sigma < 1$  in the remaining part of  $\partial S_1$ . The integral in equation (2.5) is now

$$(4.4) \quad \rho_\lambda = \text{sign}(\lambda) \int_0^1 D_\nu \sigma(x_1, q) dx_1,$$

where  $q = 0$  if  $\lambda > 0$  and  $q = 1$  if  $\lambda < 0$ . We shall now prove the theorem for  $\lambda$  positive (the proof for  $\lambda$  negative is entirely similar). It is enough to show that (the inequality here is part (ii) of Lemma A.4, proved in the appendix)

$$(4.5) \quad \rho_3 = \int_0^1 D_\nu u_3(x_1, 0) dx_1 \geq C,$$

where  $u_3$  satisfies the same equation as  $\sigma$  in the domain  $S_1$  with the boundary data

$$(4.6) \quad u_3(x_1, 1) = 1 \quad \text{and} \quad u_3(x_1, 0) = u_3(0, x_2) = u_3(1, x_2) = 0.$$

This follows because: (a) From the maximum principle  $\sigma \geq u_3$ , and (b) both  $\sigma$  and  $u_3$  vanish on  $x_2 = 0$ . Thus  $D_\nu \sigma \geq D_\nu u_3$  on the  $x_2 = 0$  side of  $S_1$ .

**4.2 Proof of Theorem 2.2**

We can decompose the solution  $\sigma$  of the problem into two parts,  $\sigma = c_j \sigma_1 + \sigma_2$ , where  $\sigma_1$  satisfies the hypothesis of the previous theorem,  $c_j$  is a constant (the size of the jump discontinuity at the origin), and  $\sigma_2$  is uniformly Hölder continuous up to the boundary, including the origin. This follows by appropriately decomposing the boundary data and then applying the results of Littman, Stampacchia, and Weinberger [12, theorem 9.1] to the existence of  $\sigma_2$ .

Notice that, from Theorem 2.1, the conjugate variable  $\eta_1$  to  $\sigma_1$  has at least a logarithmic singularity near the origin. This follows because: For any  $0 < \lambda < 1$  and any integer  $n$

$$\begin{aligned} \eta_1\left(\frac{1}{2^n}\lambda, 0\right) - \eta_1(\lambda, 0) &= \int_\lambda^{\frac{1}{2^n}\lambda} (\eta_1)_{x_1}(x, 0) dx \\ &= - \int_\lambda^{\frac{1}{2^n}\lambda} D_\nu \sigma_1(x, 0) dx \\ &= \sum_{j=1}^n \int_{\frac{1}{2^j}\lambda}^{\frac{1}{2^{j-1}}\lambda} D_\nu \sigma_1(x, 0) dx \\ &\geq nC = \left(-\log_2\left(\frac{\lambda}{2^n}\right) + \log_2(\lambda)\right) C. \end{aligned}$$

Also, since  $(\eta_1)_{x_1}(x, 0) = -D_\nu \sigma_1(x, 0) \leq 0$  for  $x > 0$ ,  $\eta_1(x, 0)$  is monotone for  $x > 0$ . Thus

$$(4.7) \quad \eta_1(x, 0) \geq C_0 |\log(x)|$$

near the origin (the same argument works for  $x < 0$ ) for some constant  $C_0 > 0$ .

Further (as follows from the results in section 6.5, part II, of [2]), the conjugate variable  $\eta_2$  to  $\sigma_2$  has a finite  $C^\alpha$  norm for some  $\alpha$  positive. Thus it is bounded. It follows that  $\eta = \eta_1 + \eta_2$  has at least logarithmic behavior near the origin. This completes the proof.

**Appendix**

In this appendix we use the harmonic measure theory of [4] to prove the lemma needed in Section 4. We shall work in the square  $S_1$  (see equation (4.2)) and consider Dirichlet problems for a uniformly elliptic symmetric operator  $\mathcal{L}$  defined as in equations (2.2)–(2.4).

**Notation and Definitions**

- $I_1, \dots, I_4$  denote the four sides of  $S_1$ , labeled consecutively in counterclockwise fashion with  $I_1$  the “lower” side corresponding to  $x_2 = 0$ .
- $G_{\vec{y}} = G_{\vec{y}}(\vec{x})$  is the *Green function* for the operator  $\mathcal{L}$  with the singularity at the point  $\vec{y}$  inside  $S_1$ . That is,  $G_{\vec{y}}$  vanishes on  $\partial S_1$  and

$$-\mathcal{L}G_{\vec{y}} = \delta(\vec{x} - \vec{y}),$$

where  $\delta$  is the Dirac delta. We note that the Green function is positive inside  $S_1$ .

- For any point  $\vec{y}$  inside  $S_1$ , the *harmonic measure* associated with  $\mathcal{L}$  is a positive measure  $\mu_{\vec{y}}$  on  $\partial S_1$  such that, given any arc  $A$  along  $\partial S_1$ ,

$$(A.1) \quad \mu_{\vec{y}}(A) = u(\vec{y}) = \int_{\partial S_1} \chi_A D_\nu G_{\vec{y}} ds .$$

Here  $ds$  is the arc length,  $\chi_A$  is the characteristic function of the set  $A$ , and  $u$  solves

$$(A.2) \quad \left. \begin{aligned} \mathcal{L}u &= 0 && \text{in } S_1 \\ u|_{\partial S_1} &= \chi_A \end{aligned} \right\} .$$

We now quote two theorems in harmonic measure theory of elliptic operators in divergence form as they apply to our situation. These results were proven by Caffarelli, Fabes, Mortola, and Salsa [4]—see theorem 2.3 (p. 631) and theorem 1.4 (p. 627), respectively.

**THEOREM A.1 (Doubling Property of the Measure  $\mu_{\vec{y}}$ )** *Given two adjacent arcs of equal length (say,  $A$  and  $B$ ) along  $\partial S_1$ :*

$$(A.3) \quad \mu_{\vec{y}}(A) \leq C_d \mu_{\vec{y}}(B)$$

for some constant  $C_d \geq 1$  that depends only on the distance from the point  $\vec{y}$  to the boundary  $\partial S_1$  and the ellipticity of the operator  $\mathcal{L}$ . That is,  $C_d = C_d(\text{dist}(\vec{y}, \partial S_1), M)$  only.

**THEOREM A.2 (Boundary Harnack Principle)** *Let  $u$  and  $v$  be positive solutions in  $S_1$  of  $\mathcal{L}\sigma = 0$ . Suppose that they vanish simultaneously along some arc  $A$  on  $\partial S_1$ . Then  $u$  and  $v$  satisfy*

$$(A.4) \quad \frac{v(\vec{x})}{u(\vec{x})} \leq C_h \frac{v(\vec{y})}{u(\vec{y})}$$

for any points  $\vec{x}$  and  $\vec{y}$  inside  $S_1$ , where  $C_h \geq 1$  is a constant that depends only on the ellipticity of  $\mathcal{L}$  and the distance from the points  $\vec{x}$  and  $\vec{y}$  to the complement to the boundary  $\partial S_1$  of  $A$ . That is,  $C_h = C_h(\text{dist}(\{\vec{x}, \vec{y}\}, \partial S_1 - A), M)$  only.

Divide the boundary  $\partial S_1$  of  $S_1$  into a sequence of  $N$  consecutive arcs of equal length. Then sequentially apply Theorem A.1 to each pair in the sequence, starting from some arbitrary member of the set. The sum of all the measures in the set must be equal to 1, thus:

COROLLARY A.3 Given  $N$  consecutive and disjoint arcs of equal length (say,  $A_1, \dots, A_N$ ) covering  $\partial S_1$ , we have

$$(A.5) \quad \mu_{\vec{y}}(A_i) \geq C_m = C_m(\text{dist}(\vec{y}, \partial S_1), M, N),$$

where  $C_m > 0$  is a constant depending only on the indicated arguments. In fact, in terms of  $C_d$  in Theorem A.1, we have  $C_m = (C_d - 1)(C_d^N - 1)^{-1}$ .

Consider now the function  $u_3$  defined in equation (4.6). That is,  $\mathcal{L}u_3 = 0$  in  $S_1$  with data  $u_3 = \chi_{I_3}$  on  $\partial S_1$ . Alternatively, we have, from equations (A.1)–(A.2):

$$(A.6) \quad u_3(\vec{x}) = \mu_{\vec{x}}(I_3).$$

LEMMA A.4 (Properties of  $u_3$ ) (i) If  $D$  is any set compactly contained inside  $S_1$ ,

$$(A.7) \quad u_3|_D \geq C_u = C_u(\text{dist}(D, \partial S_3), M),$$

where  $C_u > 0$  is a constant that depends only on the indicated arguments.

(ii) Along  $I_1$  (the interval opposite to  $I_3$ ),

$$(A.8) \quad \int_{I_1} D_\nu u_3 ds \geq C > 0,$$

where  $C = C(M) > 0$  is a constant that depends solely on the ellipticity of  $\mathcal{L}$  and  $ds$  is the arc length on the boundary.

PROOF: (i) is an immediate consequence of (A.6) and Corollary A.3 with  $A_i = I_i$  and  $N = 4$ .

For part (ii) we use Theorem A.2 on the rectangle

$$(A.9) \quad S_{1/4} = \{0 \leq x_1 \leq 1, 0 \leq x_2 \leq \frac{1}{4}\},$$

with  $u = u_3$  and  $v = G_{\vec{a}}$ . Here  $\vec{a} = (0.5, 0.5)^T$  is the center of  $S_1$ , which is outside  $S_{1/4}$ . Both  $u$  and  $v$  vanish on three sides of  $S_{1/4}$  (all but the top side, corresponding to  $x_2 = 0.25$ ). Thus we have

$$(A.10) \quad u_3(\vec{x}) \geq \frac{u_3(\vec{b})}{G_{\vec{a}}(\vec{b}) C_h} G_{\vec{a}}(\vec{x}),$$

where  $\vec{b} = (0.5, 0.125)^T$  is the center of  $S_{1/4}$ .

This last inequality is sensible as long as  $\vec{x}$  remains away from the top side of  $S_{1/4}$ . In particular, we get arbitrarily close to the bottom side  $I_1$ . Then, since both  $G_{\vec{a}}$  and  $u_3$  vanish on  $I_3$ , we get for the inner conormal derivatives along  $I_3$  the following inequality:

$$(A.11) \quad D_\nu u_3 \geq C_* D_\nu G_{\vec{a}},$$

where

$$C_* = \frac{u_3(\vec{b})}{G_{\vec{a}}(\vec{b}) C_h} > 0.$$

We note that  $G_{\vec{a}}(\vec{b})$  is bounded by a universal constant, dependent on the ellipticity of  $\mathcal{L}$  only because  $\text{dist}(\vec{a}, \vec{b})$  is fixed. Thus, using part (i), we see that  $C_* = C_*(M)$  only. Then

$$(A.12) \quad \int_{I_1} D_\nu u_3 ds \geq C_* \int_{I_1} D_\nu G_{\vec{a}} ds = C_* \mu_{\vec{a}}(I_1) = C,$$

where  $C$  has the desired properties (use Corollary A.3 on the set  $I_1, \dots, I_4$  for  $\mu_{\vec{a}}^*$ ). This concludes the proof.  $\square$

**Acknowledgments.** The authors would like to thank Luis Caffarelli for pointing out the results used in the appendix on harmonic measure. Irene M. Gamba was partially supported by NSF DMS 9623037, Rodolfo R. Rosales by NSF DMS 9311438, and Esteban G. Tabak by NSF DMS 9501073 and an A. P. Sloan fellowship.

### Bibliography

- [1] Berger, M. Private communication, 1997.
- [2] Bers, L.; John, F.; Schechter, M. *Partial differential equations*. Interscience, New York, 1964.
- [3] Brio, M.; Hunter, J. K. Mach reflection for the two dimensional Burgers equation. *Phys. D* **60** (1992), 194–207.
- [4] Caffarelli, L.; Fabes, E.; Mortola, S.; Salsa, S. Boundary behavior of nonnegative solutions of elliptic operators in divergence form. *Indiana Univ. Math. J.* **30** (1981), 621–640.
- [5] Čanić S.; Keyfitz, B. L. An elliptic problem arising from the unsteady transonic small disturbance equation. *J. Differential Equations* **125** (1996), 548–574.
- [6] Čanić, S.; Keyfitz, B. L. A smooth solution for a Keldysh type equation. *Comm. Partial Differential Equations* **21** (1996), 319–340.
- [7] Colella, P.; Henderson, L. F. The von Neumann paradox for the diffraction of weak shock waves. *J. Fluid Mech.* **213** (1990), 71–94.
- [8] Glaz, H.; Colella, P.; Glass, I. I.; Deschambault, R. L. *A detailed numerical, graphical and experimental study of oblique shock wave reflections*. Lawrence Berkeley Laboratory Report 20033, University of California, 1985.
- [9] Grüter, M.; Widman, K.-O. The Green function for uniformly elliptic equations. *Manuscripta Math.* **37** (1982), 303–342.
- [10] Hunter, J. K. Transverse diffraction of nonlinear waves and singular rays. *SIAM J. Appl. Math.* **48** (1988), 1–37.
- [11] Kenig, C.; Koch, H.; Pipher, J.; Toro, T. Area integral and harmonic measure estimates for nonsymmetric elliptic operators in divergence form. To appear in *Adv. in Math.*
- [12] Littman, W.; Stampacchia, G.; Weinberger, H. F. Regular points for elliptic equations with discontinuous coefficients. *Ann. Scuola Norm. Sup. Pisa (3)* **17** (1963), 43–77.
- [13] Morawetz, C. S. Potential theory for regular and Mach reflection of a shock at a wedge. *Comm. Pure Appl. Math.* **47** (1994), 593–624.
- [14] Reines, F.; von Neumann, J. The Mach effect and height of burst. *Collected works*, 309–347, Vol. VI, Macmillan, New York, 1963.
- [15] Rosales, R. R. Diffraction effects in weakly nonlinear detonation waves. *Nonlinear hyperbolic problems (Bordeaux, 1988)*, 227–239, Lecture Notes in Math., 1402, Springer, Berlin–New York, 1989.



- [16] Sturtevant, B.; Kulkarny, V. A. The focusing of weak shock waves. *J. Fluid Mech.* **73** (1976), 651–671.
- [17] Tabak, E. G.; Rosales, R. R. Focusing of weak shock waves and the von Neumann paradox of oblique shock reflection. *Phys. Fluids* **6** (1994), 1874–1892.
- [18] von Neumann, J. Oblique reflection of shocks. *Collected works*, 238–299, Vol. VI, Macmillan, New York, 1963.
- [19] von Neumann, J. Refraction intersection and reflection of shock waves. *Collected works*, 300–308, Vol. VI, Macmillan, New York, 1963.

IRENE M. GAMBA  
The University of Texas at Austin  
Department of Mathematics  
and TICAM  
RLM 8.100  
Austin, TX 78712-1082  
E-mail: gamba@math.utexas.edu

RODOLFO R. ROSALES  
Massachusetts Institute of Technology  
Department of Mathematics  
77 Massachusetts Avenue  
Cambridge, MA 02139  
E-mail: rrr@math.mit.edu

ESTEBAN G. TABAK  
Courant Institute  
251 Mercer Street  
New York, NY 10012-1185  
E-mail: tabak@cims.nyu.edu

Received November 1997.